ISSN 0010-9525, Cosmic Research, 2016, Vol. 54, No. 3, pp. 205–216. © Pleiades Publishing, Ltd., 2016.
Original Russian Text © V.N. Marichev, D.A. Bochkovskii, I.V. Sorokin, V.V. Bychkov, 2016, published in Kosmicheskie Issledovaniya, 2016, Vol. 54, No. 3, pp. 217–228.

Estimation of Potential Abilities of Middle Atmosphere Density Measurements from a Near-Earth Orbit within the UV Wavelength Range

V. N. Marichev[a, b], D. A. Bochkovskii[a, b], I. V. Sorokin[c], and V. V. Bychkov[d]

[a] *Zuev Institute of Atmospheric Optics, Siberian Branch, Russian Academy of Sciences, Tomsk, Russia*

[b] *National Research State University, Tomsk, Russia*

[c] *Korolev Rocket and Space Corporation Energia, Korolev, Russia*

[d] *Institute of Cosmophysical Research and Radiowave Propagation, Far Eastern Branch, Russian Academy of Sciences, Kamchatka Region, Elizovskii District, Paratunka, Russia*

Received March 13, 2014

Abstract—Analysis of errors in atmospheric density measurements by lidar on board the ISS is performed. It is shown that using as the lidar transmitter a Nd:YAG laser with moderate parameters of emission at a wavelength of 353 nm and a receiving mirror diameter of 0.4 m, it is possible to cover with a 10% measurement error a height range, on average, from 40–60 km and 30–40 km in the nighttime and daytime, respectively, down to the troposphere. Working with emission at 266 nm with a 10% error, it is possible to move to the heights of the mesosphere (70 km) and penetrate the atmosphere down to a height of 40 km. Thus, the use of two harmonics makes it possible to assimilate the height range of atmospheric density measurements from on board the ISS beginning from 70 km and down to the troposphere.

DOI: 10.1134/S0010952516030047

1. INTRODUCTION

The air density, together with temperature, pressure, and humidity, is one of the main meteorological characteristics of the atmosphere. It is subjected to exponential decrease with height in the atmosphere within a large dynamic range from 1.2–1.3 g m^{-3} at ground level to 5×10^{-4} g m^{-3} at a height of 100 km [1].

To solve some scientific and applied problems, real-time information on the real vertical distribution of atmospheric density is needed. It is important, in particular, for high-accuracy handling motion of space vehicle (SV) capsules in dense atmospheric layers. Descent to Earth modules (DM) of manned spacecrafts and interplanetary stations enter the atmosphere with the first or second space velocity. In order to eliminate that velocity due to atmospheric drag for manned or ballistic descent and soft landing, the character of atmospheric density oscillations must be known. Even small deviations in the density values at heights corresponding to the so-called entrance corridor lead to a substantial change in the calculated trajectories and an increase in overloading, substantial thermal loading, and even mechanical damage to a DM [http://astroera.net/content/view/396/9/].

In calculating the parameters of DM motion, the unified, so-called standard atmosphere is commonly used. Currently, in Russia, the standard atmosphere (GOST 4401-81) providing numerous values of the main thermodynamic and physical parameters of the air medium at heights up to 200 km (independently of time of year, day, and geographic location) is accepted and used for simulation. However, due to the unpredictable behavior of the density profile values, its calculation accuracy is obviously insufficient. For example, in the 1960s–1970s, for each flight of *Zond* SVs, the *Voeikov* and *Shakal'skii* research vessels traveled into the Indian Ocean region and provided atmospheric sounding with the help of meteorological rockets not long before SV entrance into dense atmospheric layers. Based on the measurements results, information containing special corrections based on the actual state of the atmosphere was transmitted. These measures were important for the successful flights of these SVs ([http://www.walkinspace.ru/blog/2010-12-02-282]).

Conducting measurements of atmospheric density using rocket launches (as can be seen from the presented example) is a one-time and expensive measure. For these aims, we propose an alternate version: lidar methods and atmospheric sounding tools. Development of lidar technologies has led to their broad use in studying the composition and properties of the middle

atmosphere both in Russia and abroad. The best lidar technology in the world is concentrated at the NDACC (Network for the Detection of Atmospheric Composition Change) [http://www.ndsc.ncep.noaa.gov/]. Regular observations of stratospheric and tropospheric ozone, temperature, aerosol, and stratospheric clouds are carried out at the more than 20 stations of this network [2, 3]. In Russia, such studies are carried out at lidar stations of Russian Academy of Sciences (RAS) institutes in Tomsk, Yakutsk, Petropavlovsk-Kamchatskii, and Vladivostok. The devices installed at these stations also make it possible to observe ozone, temperature, and aerosol in the stratosphere and mesosphere [4–16]. However there are no targeted or systematic studies of atmospheric density variations abroad or in Russia. Using numerical simulations, we analyzed the potential of lidar measurements of the air density in the middle atmosphere within the visible wavelength range on board an SV located in a near-Earth orbit [17]. The calculations were performed for a lidar with fairly moderate technical characteristics: the transmitter is the solid-body Nd:YAG laser with an emitting wavelength of 532 nm, a pulse energy of 0.8 J, and emitting frequency of 20 Hz. For the receiving system, the main mirror has a radius of 0.3 and 0.5 m, the field of view is 0.1 and 1 μrad, and the spectral width of the light filter is 0.5, 1, and 10 nm. The time of signal accumulation was 10 min for a vertical spatial resolution of 1 km. Three versions of sounding were considered: from the surface of the Earth, from aircraft, and from on board the ISS at an orbit of 414 km. In particular, it was shown that for the standard deviation of 10% for space-based observations, it was possible to reach a height interval up to 55 km in the daytime and up to 70 km at night.

To further develop methods and tools for lidar studies of the atmosphere from on board an SV, it is feasible to switch from the visible to the ultraviolet range. The latter is interesting due to the stronger interaction of radiation with the molecular atmosphere as a scattering medium: proportional to the fourth degree of wavelength ratio within the visible and UV ranges. The third (355 nm) and fourth (266 nm) harmonics of the Nd:YAG laser widely used in lidar technologies—for which currently the maximum energy radiated in a pulse is obtained—were considered for atmospheric sounding. At the chosen wavelengths, the interaction intensity would be higher by a factor of 5 and 16 compared to 532 nm. Therefore, the lidar signal power would be higher by the same factors. However, at the same time, it should be taken into account that their attenuation in the UV range due to molecular scattering would be higher. For radiation at 266 nm, absorption by ozone should also be taken into account. Mainly, we considered UV range in order to increase the efficiency of measurements from space due to the substantial increase in lidar signal power.

2. LIDAR SIGNAL AND NOISE COMPONENTS

The lidar signal power is described by the laser sounding equation, which has the following form in the single elastic scattering approximation of light for reception of radiation in the photon count mode:

$$N_{\mathrm{L}}(H,\Delta H) = \eta E_0/h\nu \cdot T_{\mathrm{app}} \cdot A\Delta H/H^2 \times T_M^2(H)T_{\mathrm{a}}^2(H) \cdot [\beta_{M\pi}(H) + \beta_{\mathrm{a}\pi}(H)],$$

where N(H, ΔH) is the number of photons received from height H within interval ΔH, E0 is the energy of the emitted laser pulse, hν is the energy of one photon at the laser wavelength, η is the quantum efficiency of the photoreceiver, Tapp is the transmission of the receiving–emitting optical tract of the lidar, A is the area of the lidar receiving aperture, $T_{\mathrm{M}}^2(H)$, and $T_{\mathrm{a}}^2(H)$ are the transmission of radiation by an atmospheric layer to a sounding object at distance H and back, respectively, and βMπ(H) and βaπ(H) are coefficients of backscattered molecular and aerosol scatter of laser emission, respectively. During sounding from the space, height H should mean the difference between the values of the SV's orbit height and the height of the sounded atmospheric region over the Earth's surface, $H_{\mathrm{or}} - H$.

$$N_\Sigma(H,\Delta H) = N_{\mathrm{L}}(H,\Delta H) + N_{\mathrm{B}} + N_{\mathrm{D}}.$$

Here

$$N_{\mathrm{B}} = T_{\mathrm{app}}\eta B S_{\pi i}\Omega_i/h\nu \cdot 2\Delta H/c \cdot \Delta\lambda_i P(H_{\mathrm{or}} - H),$$

where Tapp,tr is the transmission of the receiving system, $P(H_{\mathrm{or}} - H)$ is the transparency of the atmospheric layer $H_{\mathrm{or}} - H$, Δλi is the passband of the light filter, B is the brightness of the Earth's surface in the direction to the lidar, Sπi is the area of a spot on the surface cut by the lidar array's field of view, and Ωi is the solid angle of the field of view from the Earth's surface to the receiving array of the lidar.

$$B = E \cdot A_{\mathrm{E}}/\pi,$$

where E and A_{E} are the illumination and albedo of the underlying surface, respectively; $S_{\pi i} = \pi\gamma_i^2(H) \cdot H_{\mathrm{or}}^2$, where γ$i$ is the linear angle of the field of view of the receiving system; $\Omega_i = \pi R_i^2/2\pi H_{\mathrm{or}}^2$, where Ri is the radius of the receiving mirror of the lidar; $N_{\mathrm{T}} = 2\Delta H/c \cdot f_{\mathrm{D}}$, where fD is the arrival rate dark current pulses.

In series of observations, the total signal from the photo receiver will be written as

$$N_\Sigma(H,\Delta H,\Delta t) = [N_L(H,\Delta H) + N_B + N_D]f\Delta t,$$

where Δt is the time of measurements and f is the sending frequency of the laser pulses.

The error in measurement of the lidar signal will be determined by the total contribution of the proper shot noise and background and dark current noise, i.e. by the Poisson statistics according to the formula

$$\delta N(H)/N(H) = (N(H) + N_B + N_D)^{1/2}/N(H).$$

3. FORMULAS FOR CALCULATION OF THE DENSITY AND ROOT-MEAN-SQUARE ERROR OF MEASUREMENTS

In the case when aerosol is absent on the sounding path, which is typical of altitudes higher than 20–30 km, the lidar signal will be proportional to the value of the molecular backscatter and therefore to the air density. Thus, in clean molecular atmosphere, it is possible to follow changes in the atmospheric density at various heights directly from lidar signals. The atmospheric density ρ is related to the backscatter molecular coefficient and the power of the lidar signal by particular constants:

$$\rho(H) = \text{const}_1 \cdot \beta_{\pi M}(H) = \text{const}_2 \cdot N_L(H)/H^2.$$

In this case, it is assumed that the transparency of the atmospheric layer above 20 km is 1, whereas emission attenuation occurs almost completely at heights below 20 km, and the $T_M^2(H)$, value is a constant included in const_2. The value of const_2 could be determined by calibration at a particular height for which the value of the air density is known. As a rule, it is the 20–30 km height range where aerosol is absent and the atmospheric density data could be obtained from the radiosonde measurements. Then the atmospheric density profile could be calculated using the simple formula:

$$\rho(H) = N_L(H)\cdot H^2/N_L(H_c)\cdot H_c^2\cdot\rho(H_c),$$

where H_c is the calibration height.

The rms measurement error is determined by the formula

$$\frac{\delta\rho}{\rho}(H) = \left\{\frac{N_L(H_c)+N_B+N_D}{[N_L(H_c)]^2} + \frac{N_L(H)+N_B+N_D}{[N_L(H)]^2}\right\}^{1/2}.$$

4. SOUNDING AT A WAVELENGTH OF 355 nm

4.1. Initial Data

The lidar signal power were calculated for two apertures with a radius of 0.2 and 0.5 m within the 0–100 km height interval for the following input parameters: quantum efficiency of the receiver $\eta = 0.2$, laser pulse energy $E_0 = 0.4$ J, photon energy at a wavelength of 353 nm $h\nu = 5.63\times10^{-19}$ J, transmission of receiving–transmitting tract $T_{app} = 0.2$, spatial resolution $\Delta H = 1$ km, and pulse transmission frequency $f = 20$ Hz. The signal accumulation time $\Delta t_1 = 60$ s, $\Delta t_2 = 12$ s, which corresponds to the horizontal spatial resolution of the measurements of 460 and 90 km, respectively, by the lidar installed on board ISS with the orbit height of 390 km. The lidar signals (scattering, attenuation) were calculated using the atmospheric model [18].

The background signal value was calculated for the receiving system transmission $T_{app,tr} = 0.3$ for two values of the transmission width of the interference filters and two fields of view of the receiving telescope: $\Delta\lambda_1 = 1$ nm, $\Delta\lambda_2 = 0.04$ nm; $\gamma_1 = 0.5$ μrad, $\gamma_2 = 0.2$ μrad.

In estimating the background exposure, according to the data from [19], the illumination of the surface in the daytime was $E = 0.5$ W m^{-2} nm^{-1}. Values of 0.9, 0.5, 0.1, 0.01, and 0.001 imitating measurements in the daytime, twilight, and nighttime periods were introduced for the albedo. Moreover, we introduced a correction to the background exposure from the solar radiation scattered by the atmosphere at 10% exposure provided by reflected solar radiation. For the nighttime conditions (under the Moon), according to [http://about-space.ru/rasseyanscet?start=41], illumination by moonlight was determined with a value of 0.0002–0.0003% of the Sun's illumination (the corresponding imitating values of the albedo were 3×10^{-6}, 1.5×10^{-6}, and 1×10^{-6}, respectively). Calculating the dark component of noise, the arrival rate of dark photo pulses was $f_D = 50$ pulses/s.

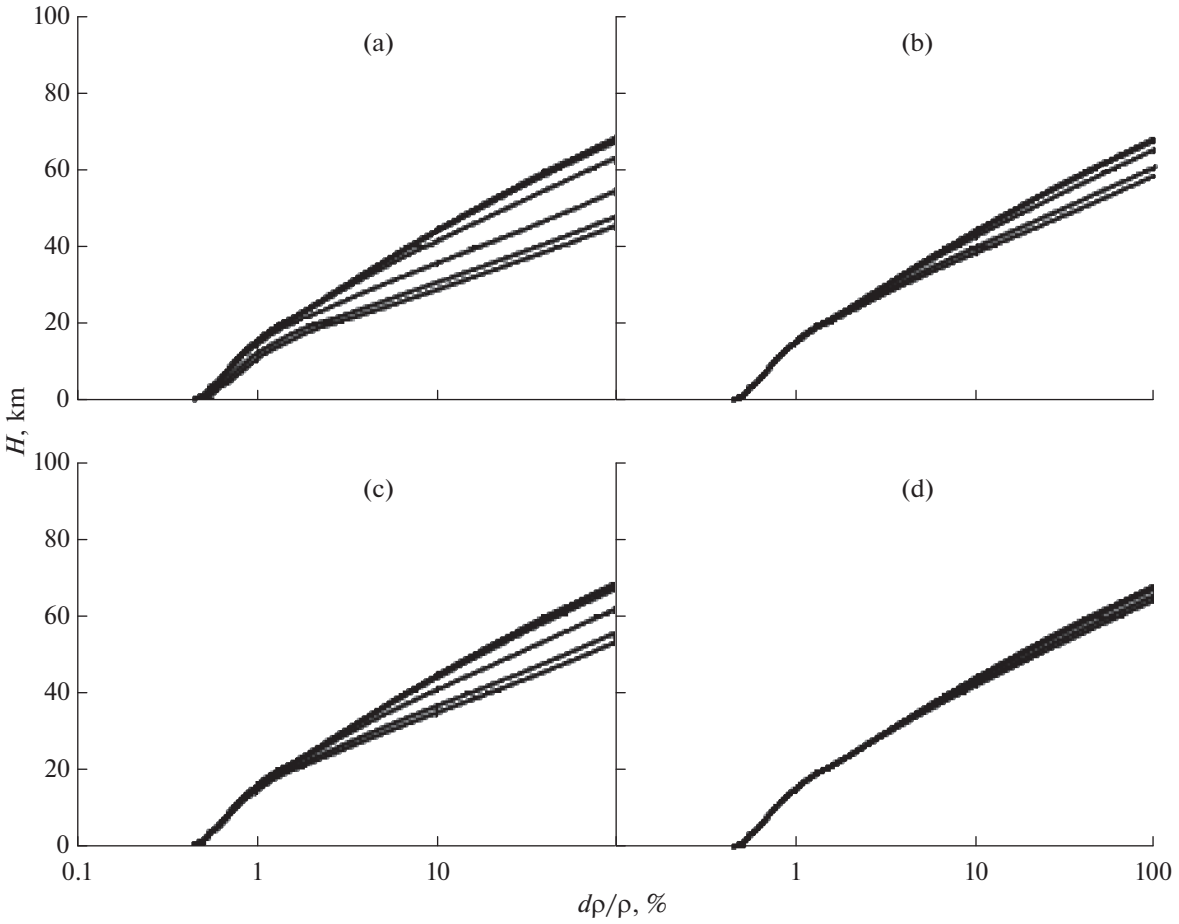

Fig. 1. Root-mean-square deviation of atmospheric density measurements with receiving aperture radius of 0.2 m for field view of 1 (a, b) and 0.1 (c, d) μrad. The horizontal spatial resolution is 90 km.

4.2. Results of Calculations of Errors in Atmospheric Density Measurements

The accuracy characteristics of the atmospheric density measurements by the space-based lidar at a wavelength of 355 nm are shown in Figs. 1–4. The first two and last two figures show measurements with the receiving mirror with a radius of 0.2 and 0.5 m, respectively, conducted for two accumulation time values of 12 and 60 s and different transmission width of light filters and fields of view (see above). In all figures, the network of curves from bottom to top is given in order of decreasing illumination from the maximum values in the daytime to the minimum values at night.

Figure 1 shows the measurement errors for a signal accumulation time of 12 s. One can see that for a field of view of 0.5 μrad under daytime illumination conditions (Figs. 1a, 1b), atmospheric density could be measured with acceptable accuracy (the error is 10%) from 30 ($\Delta\lambda = 1$ nm) and 40 km ($\Delta\lambda = 0.04$ nm) down to the Earth's surface. However, as noted above, it is the very same range in which the presence of the aerosol component, at least below 20 km, makes it methodically impossible to conduct reliable atmospheric density measurements. In twilight and evening time, the "ceiling" of the 10% error level increases from 35 to 40 km depending on the width of the light filters. In this case, the 20–40 km height range where measurements are methodically correct is covered. At night, measurements can be conducted beginning from heights above 40 km.

The measurement accuracy is substantially improved for a narrower field of view of 0.2 μrad. In the daytime, twilight, and evening time, and at night, measurements could be conducted from heights of 37–40 km, 40 km, and approximately 45 km, respectively. The rms decreases rapidly with height and at the 20 km level does not exceed 2–3% percent for the daytime conditions, whereas it is less than 1% below 20 km.

An increase in the signal accumulation time up to 60 s results in an increase in the sounding ceiling by a few kilometers (Fig. 2). Thus, for the field of view of 0.5 μrad and the 1 nm width of the light filter passband

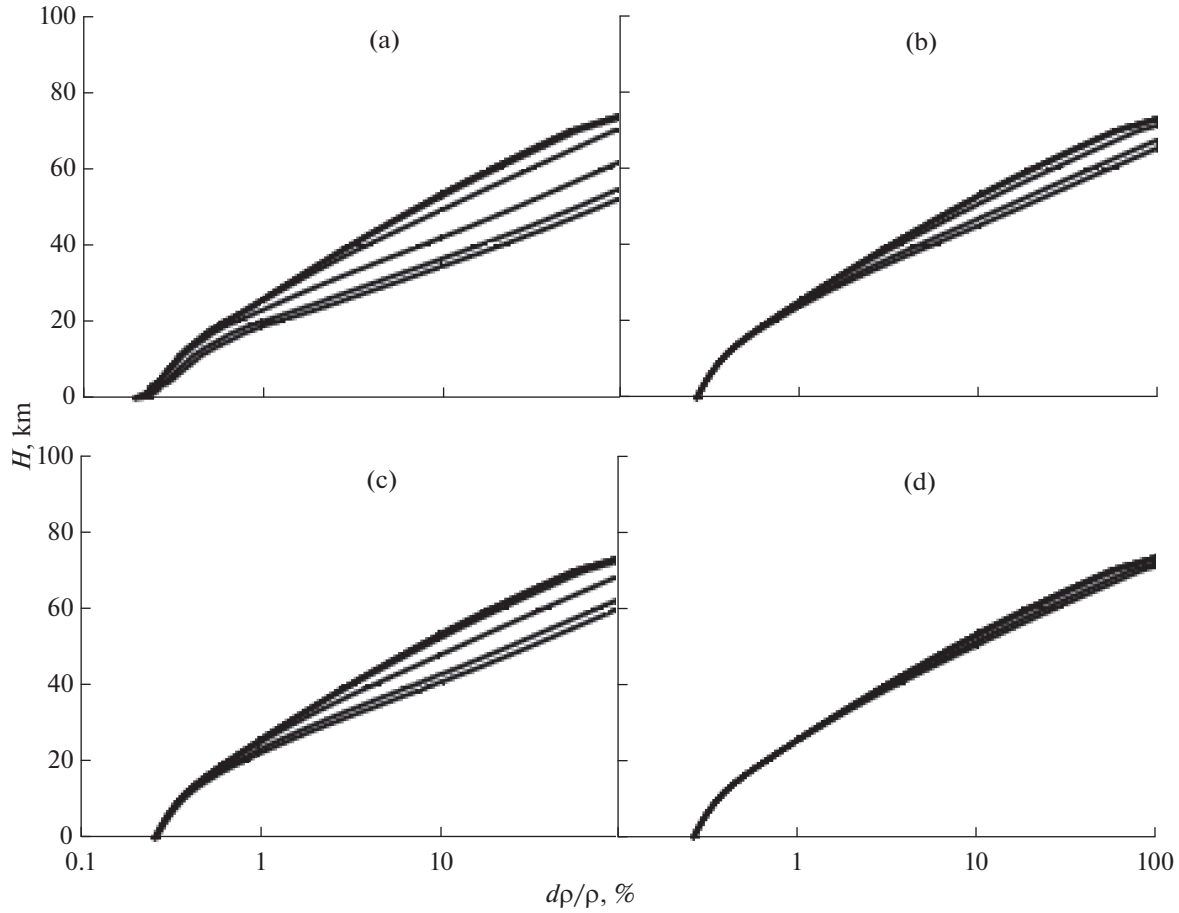

Fig. 2. Same as in Fig. 1 but for horizontal spatial resolution of 460 km.

(Fig. 2a), the 10% level of measurement error can be reached at 35, 42, and 57 km in the daytime, at twilight and evening, and at night, respectively. The corresponding values for the light filter with a bandwidth of 0.04 nm (Fig. 2b) are 45–47 km depending on the time of the day.

For a decrease in the field of view of the receiving system down to 0.2 μrad (Figs. 2c, 2d), measurements with the 10% error level can be conducted beginning from 40 ($\Delta\lambda$ = 1 nm) and 50 km ($\Delta\lambda$ = 0.04 nm) in the daytime, from 47 ($\Delta\lambda$ = 1 nm) and 50 km ($\Delta\lambda$ = 0.04 nm) at twilight and evening, and from 55 km at night. Below these heights, the measurement accuracy increases rapidly assuming the absence of aerosol on the path.

A receiving mirror with a larger radius of 0.5 m (Figs. 3, 4) for both fields of view of 0.5 and 0.2 μrad leads, due to the increase in the lidar signal power, to widening of the measurement height range for a width of the light filter passband of both 1 and 0.04 nm, on average, by 5–10 km over the illuminated surface of the Earth; it increases up to 15 km for measurements over the dark surface. For the 10% error level, the atmospheric density with such a receiving mirror can be measured beginning from heights of 35–55 km in the daytime (depending on the field of view and passband of the light filters) and from 60 km at night for a 12 s signal accumulation time. At a 60 s signal accumulation time, the initial measurement height increases, on average, by 5–7 km. However, in this case. one should bear in mind that installation of large-sized optical equipment on board an SV presents certain difficulties.

5. SOUNDING AT A WAVELENGTH OF 266 nm

5.1. Initial Data and Peculiarities of Sounding

For atmospheric sounding at a wavelength of 266 nm, the initial data are identical to the above-mentioned case of using lidar with a laser emitting at a wavelength of 355 nm. The difference was only in an energy of an emission quantum at a wavelength of 266 nm of $h\nu = 7.4 \times 10^{-19}$ J and zero illumination of the Earth's surface.

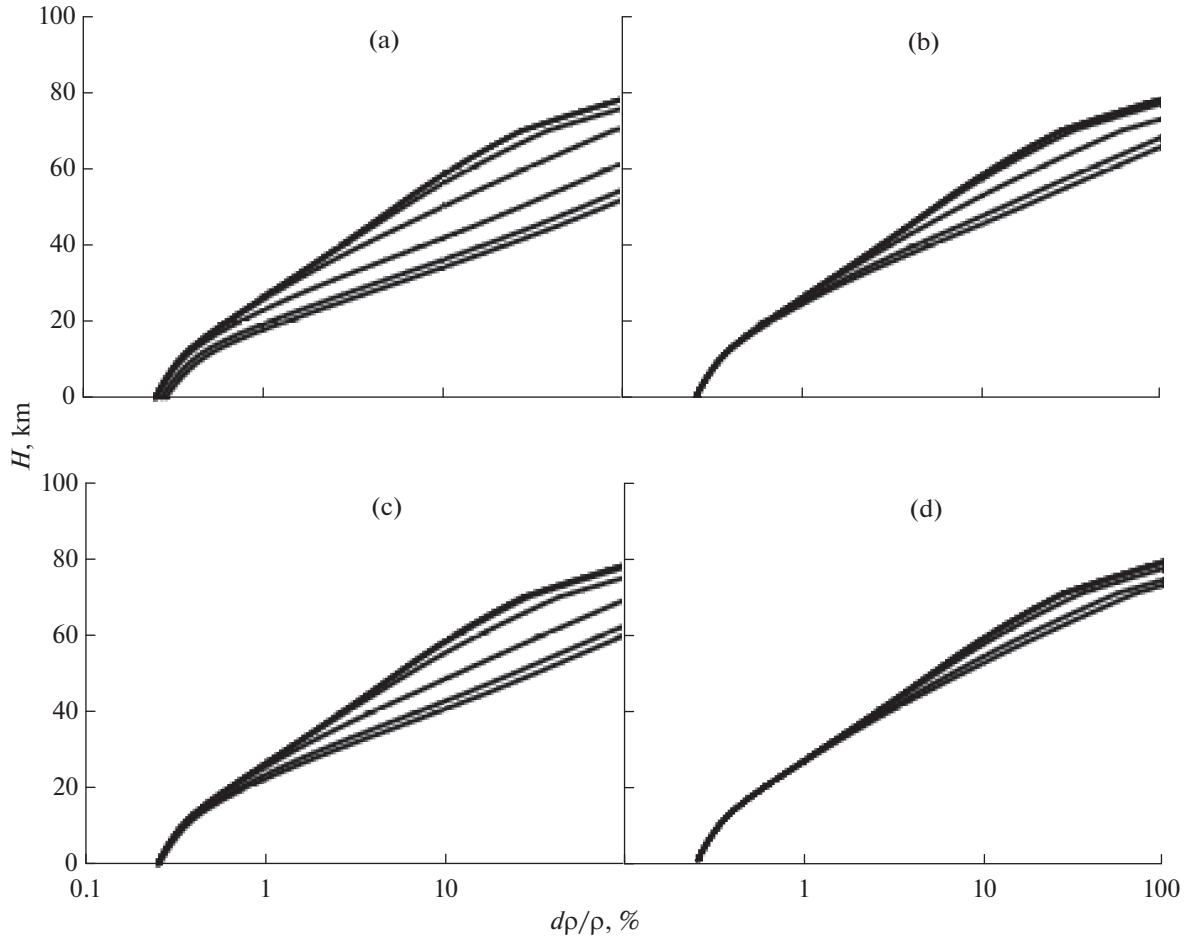

Fig. 3. Same as in Fig. 1 but for receiving mirror with radius of 0.5 m.

More intense interaction of the emission to the molecular atmosphere as a scattering medium is, as noted above, an advantage of sounding at a wavelength of 266 nm. This interaction is 16 times more intense than sounding at a wavelength of 532 nm and results in a proportional increase in the lidar signal intensity. Moreover, and no less importantly, due to absorption by stratospheric ozone, emission within this spectral range does not reach the Earth's surface and, therefore, there are no background exposures by the reflected solar radiation from the Earth's surface. In contrast, namely, due to the location of emission at a wavelength of 266 nm almost in the center of the intense Hartley ozone absorption band, strong weakening of lidar signals within the location region of the ozone layer should be expected. In order to take into account the laser emission absorption by ozone, data on the vertical distribution of its concentration taken from [20] were used. The absorption cross section of ozone at a wavelength of 266 nm was taken from [21]: 947×10^{-20} cm^2 mol^{-1}.

5.2. Results of Calculations of Errors in Atmospheric Density Measurements

Figures 5 and 6 show calculations of the standard deviation profiles of lidar atmospheric density measurements at a wavelength of 266 nm. Figure 5, which gives the calculations for a signal accumulation time of 12 s, shows that measurements with an error level below 10% are possible using the lidar with a mirror with a radius of 0.2 and 0.5 m within height intervals of 60–45 km and 75–42 km, respectively. Since the laser emission penetrates deeper into the atmosphere, the measurement accuracy increases and reaches a maximum at a height of 50 km, being a few percent. At lower altitudes, laser emission absorption by ozone begins to influence and limits lidar atmospheric density measurements from below. For a signal accumulation time of 60 s (Fig. 6), the height range of lidar measurements of the atmospheric density broadens from 70 to 42 km and from 80 to 40 km for mirrors with radii of 0.2 and 0.5 m, respectively. Thus, using shorter wave sounding UV radiation with a wavelength of

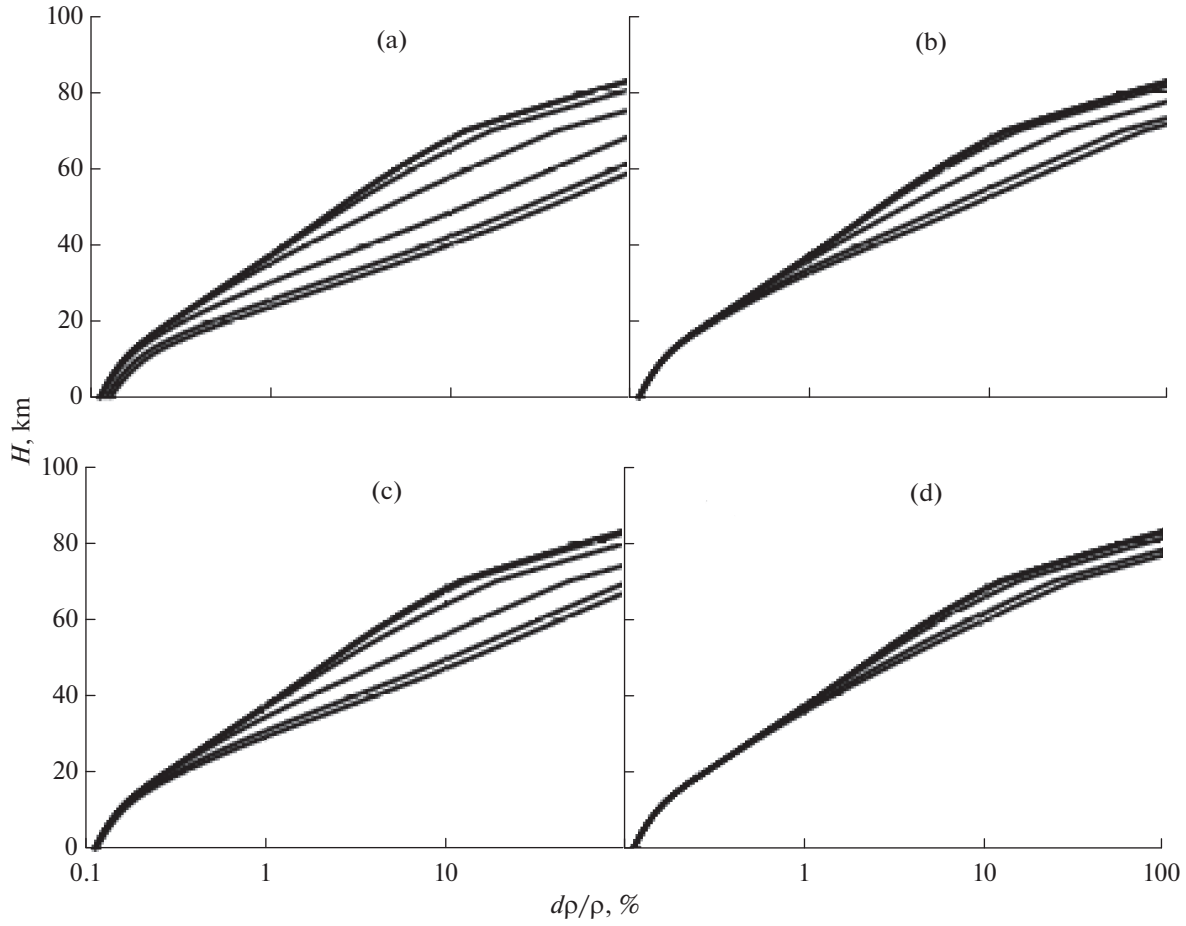

Fig. 4. Same as in Fig. 2 but for receiving mirror with radius of 0.5 m.

266 nm makes it possible to penetrate into higher atmospheric layers: into the mesosphere. At the same time, unlike for emission at a wavelength of 355 nm, the height range of measurements shown in Figs. 5 and 6 is realized independently of time of the day.

6. ALLOWANCE FOR THE INFLUENCE OF AEROSOL PRESENT IN THE MIDDLE ATMOSPHERE

As noted above in Section 3, lidar atmospheric density measurements are correct only in the absence of aerosol component in the atmosphere ($\beta_{\alpha\pi}(H) = 0$). However, actually, in the lower half of the stratosphere, it is necessary to take into account the presence and possible appearance of such aerosol formations as the Junge layer, volcanic clouds, and polar stratospheric clouds, as well as noctilucent clouds and meteor dust in the mesosphere. This could lead to distorted results when calculating atmospheric density using lidar signals.

The Junge aerosol layer is a layer of sulfuric oxide aerosol at heights from 15 to 23 km [22]. It is a remnant volcanic aerosol. It is formed due to volcanic activity, when sulfuric gas is ejected into the stratosphere, where it is oxidized and forms microdrops of sulfuric acid with a concentration level of 0.1–1 drop cm^{-3} [23]. Due to the eruptive nature of its formation, the intensity of this layer depends on volcanic activity and could decrease down to the zero level in the long absence of the latter. For example, according to lidar observations in recent years, this layer has not been recorded over Tomsk [12].

Volcanic aerosol clouds are localized within a broadened height interval from 10 to 30 km. The coefficient of the aerosol backscatter in them, as shown by the experience of lidar studies of ejections into the stratosphere at Pinatubo [24, 25], could be by tens of times higher than the molecular backscatter coefficient within the visible wavelength range and several times higher than within the UV range. This is why atmospheric density measurements are impossible in an altitude region where eruptive clouds are present.

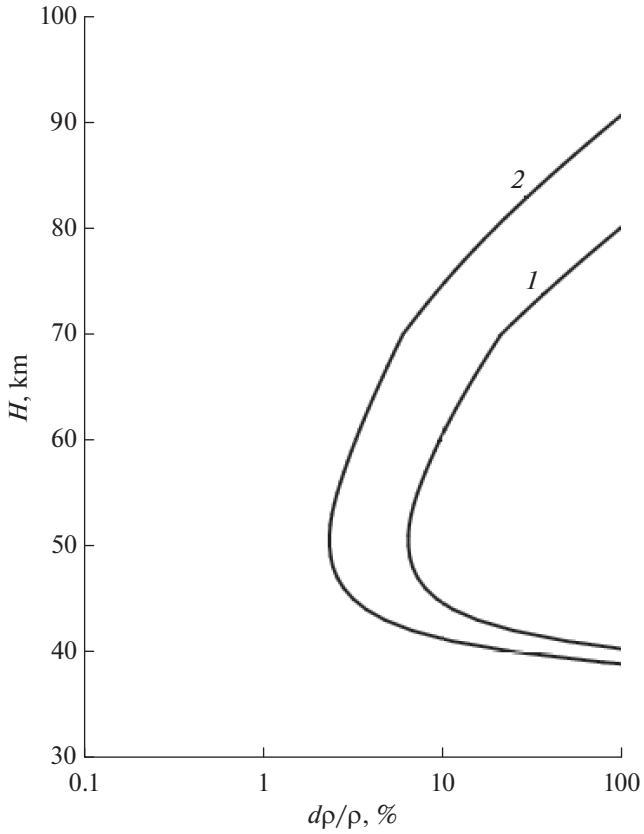

Fig. 5. Root-mean-square deviation of atmospheric density measurements with receiving aperture radius of 0.2 (curve *1*) and 0.5 m (curve *2*) at wavelength of 266 nm. The horizontal spatial resolution is 90 km (the signal accumulation time is 12 s).

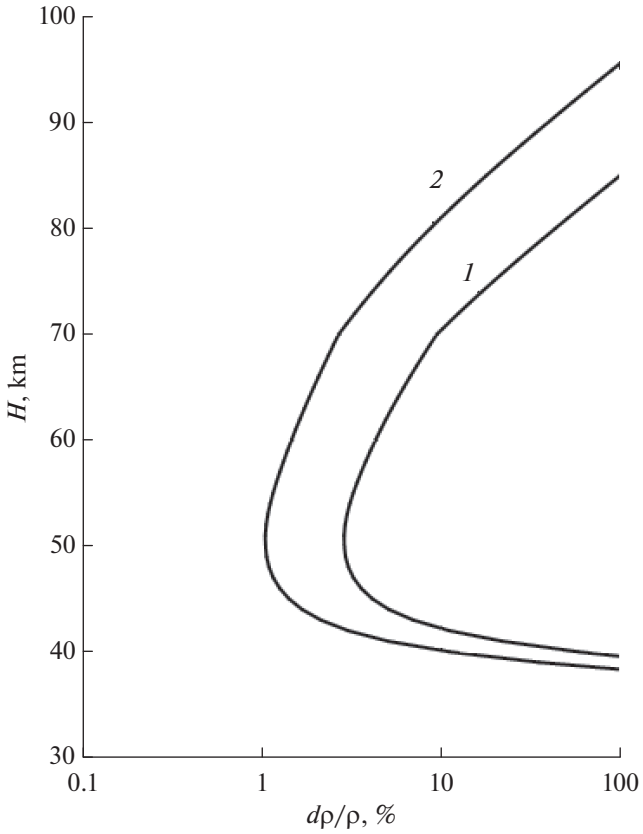

Fig. 6. Same as in Fig. 5, but for horizontal spatial resolution of 460 km (the signal accumulation time is 60 s).

Approximately the same is correct for polar stratospheric clouds, which could be located at heights from 15 to 25 km. The excess aerosol scatter over the molecular one is in them slightly lower as compared to the eruptive clouds and reaches a few units within the visible wavelength range [26].

The noctilucent clouds are formed in the mesosphere at heights of the upper mesosphere–lower thermosphere between 75 and 90 km [27]. It is a narrow aerosol layer with a very small optical thickness. However the aerosol scatter in it exceeds the molecular one by tens and hundred times and that makes it impossible to conduct measurements of the atmospheric density. The noctilucent clouds in the form of two layers located at heights of 78 and 88 km were observed over Tomsk during a long period from June to September 2008 and during one night on July 4, 2011, at a height of 80 km [28, 12].

As for the aerosol formations caused by meteors in the mesosphere, there is no data on their optical and physical parameters in the literature, so it is impossible to estimate their influence on the measurements accuracy in advance. Nevertheless, detection of the possible appearance of meteor dust in the mesosphere is possible by the lidar method. It was shown in [30] by the example of observation of meteor dust of the Chelyabinsk bolide.

According to the above-said, for lidar atmospheric density measurements, the height interval where aerosol is present should be excluded from consideration. To do that, the aerosol vertical stratification profile is determined from the same lidar observations using the method described in [29]. The optical characteristics $R(H)$, the aerosol scattering ratio, is used as the parameter describing aerosol vertical stratification. By definition, $R(H)$ is the ratio of the sum of the aerosol and molecular backscatter coefficients to the molecular backscatter coefficient. At the same time, the total and molecular scattering coefficients are determined directly from the lidar measurements and from the atmospheric model, respectively. In the presence and absence of aerosol at some height, $R(H) > 1$ and $R(H) \sim 1$ with an accuracy to the measurement error. Using the $R(H)$ value, the contribution of aerosol scattering to the total

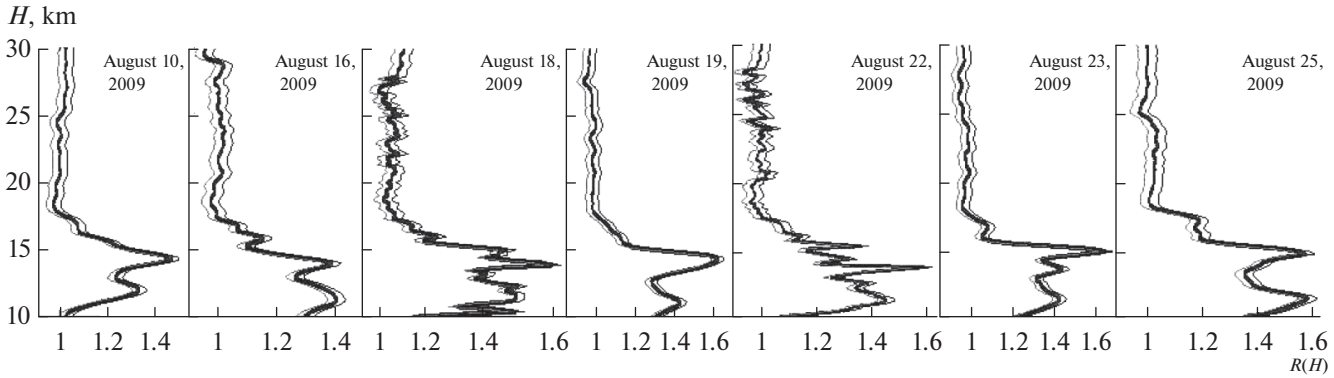

Fig. 7. Observations of passage of aerosol layer from Sarychev volcano over Tomsk on particular nights of September 2009. The edge curves mark the corridor of the rms error in measuring the scattering ratio *R(H)* [14].

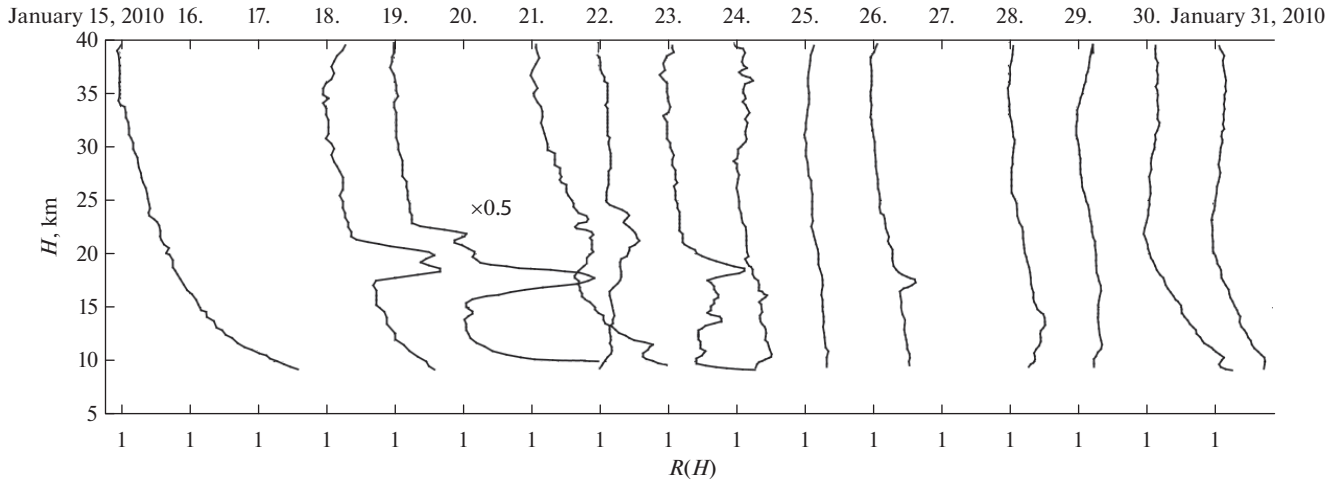

Fig. 8. Recording of transport of polar stratospheric clouds over Tomsk in period of January 18–23, 2010. The aerosol scatter for the January 19, 2010, profile is reduced by a factor of 2 to avoid overlapping with the profiles following it [31].

scattering is determined and the value of the aerosol component is estimated indirectly.

According to [29], the rms error in measuring $R(H)$ will always be less than the error in determining the atmospheric density presented in Section 3 due to the increase in the lidar signal caused by the extra aerosol scatter. The sensitivity to recording of the aerosol component within particular height intervals can be estimated using the calculated density plots in Figs. 1–6. It becomes evident that it is conservatively enough to measure the stratification of such aerosol formations as volcanic, polar, and noctilucent clouds, in the formation zone of which the aerosol scattering exceeds molecular scattering by several, tens, or hundreds of times. For a substantial aerosol content in the Junge layer and meteor dust layers, which could distort atmospheric density calculations, their vertical stratification is also completely achieved using lidar measurements.

Figures 7–11 show examples of ground-based lidar measurements of the vertical structure of volcanic and polar clouds and recording of noctilucent clouds, meteor dust layers, and the disappearance of the Junge layer.

7. CONCLUSIONS

Our analysis showed that lidar atmospheric density measurements in the UV spectral range from space make it possible to obtain more exact results within the broadened height range than measurements within the visible range. For example, for lidar sounding of the middle atmosphere on board the ISS:

1. A wavelength of 266 nm makes it possible to conduct air density measurements beginning from mesospheric heights (approximately 70–80 km); measurements completely cover the entire upper stratosphere (down to heights of 40 km). The measurement error at

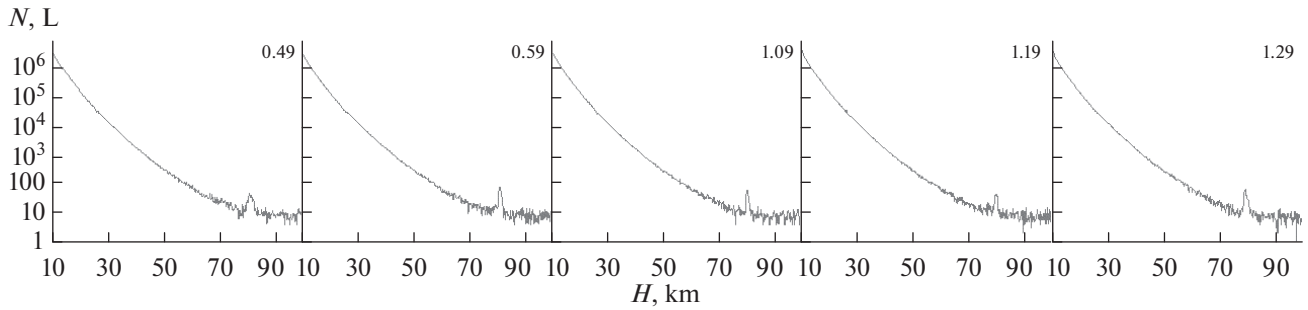

Fig. 9. Lidar observations of noctilucent clouds over Tomsk on night of July 4, 2011. The lidar signal as a number of one-electron pulses is shown on the ordinates. Each plot shows the local observation time in 10-min series. One can see that the noctilucent clouds are stably localized at a height of 80 km and their thickness varies from 2 to 3 km [11].

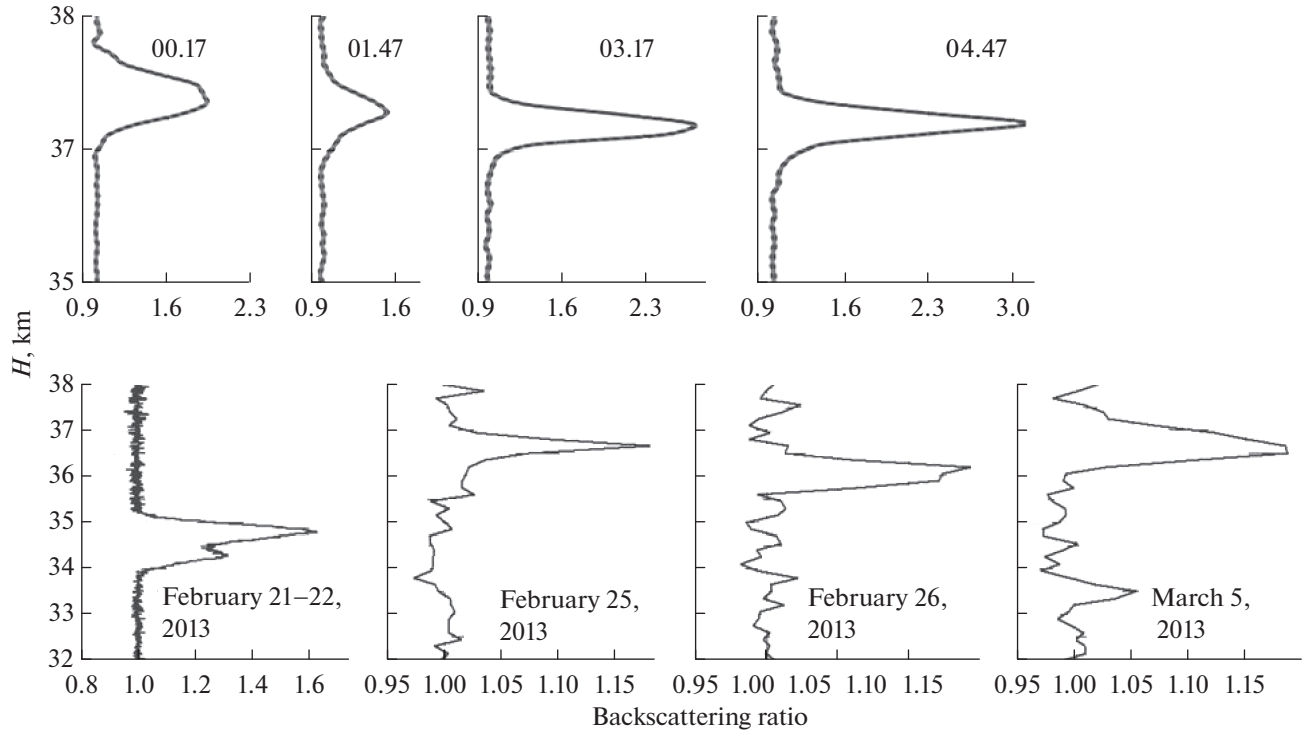

Fig. 10. Dynamics of changes in structure of aerosol layer formed by Chelyabinsk meteorite observed by lidars over Obninsk during night of February 24–25, 2013, with signal accumulation time of 1 h (top series of plots) and over Moscow on February 21–22, 2013, with averaging over the night and for following dates with averaging over 1 h (bottom series of plots). Sounding results show that the peak of meteor dust concentration was within the 35–38 km height interval [29].

the upper boundary lies within the limits 10–20% (depending on the mirror diameter and signal accumulation time), decreases with altitude, and reaches a minimum (a few percent) at a height of approximately 50 km.

2. A wavelength of 355 nm makes it possible to measure air density with an error less than 10% beginning from heights of 40–60 km (depending on the mirror diameter, time of the measurements, and time–spatial selection of signals) on the dark side of the Earth, this error decreasing with heights down to 1% or lower in the lower stratosphere.

3. Application of lidar with the transmitter operating simultaneously at wavelengths of 266 and 355 nm and with one receiving telescope solves the problem of density measurements of the upper and middle atmosphere within the range from 80 to 10–20 km (the lower boundary height depends on the presence and concentration of aerosol in the atmosphere) with an error that decreases with height. In this case, measure-

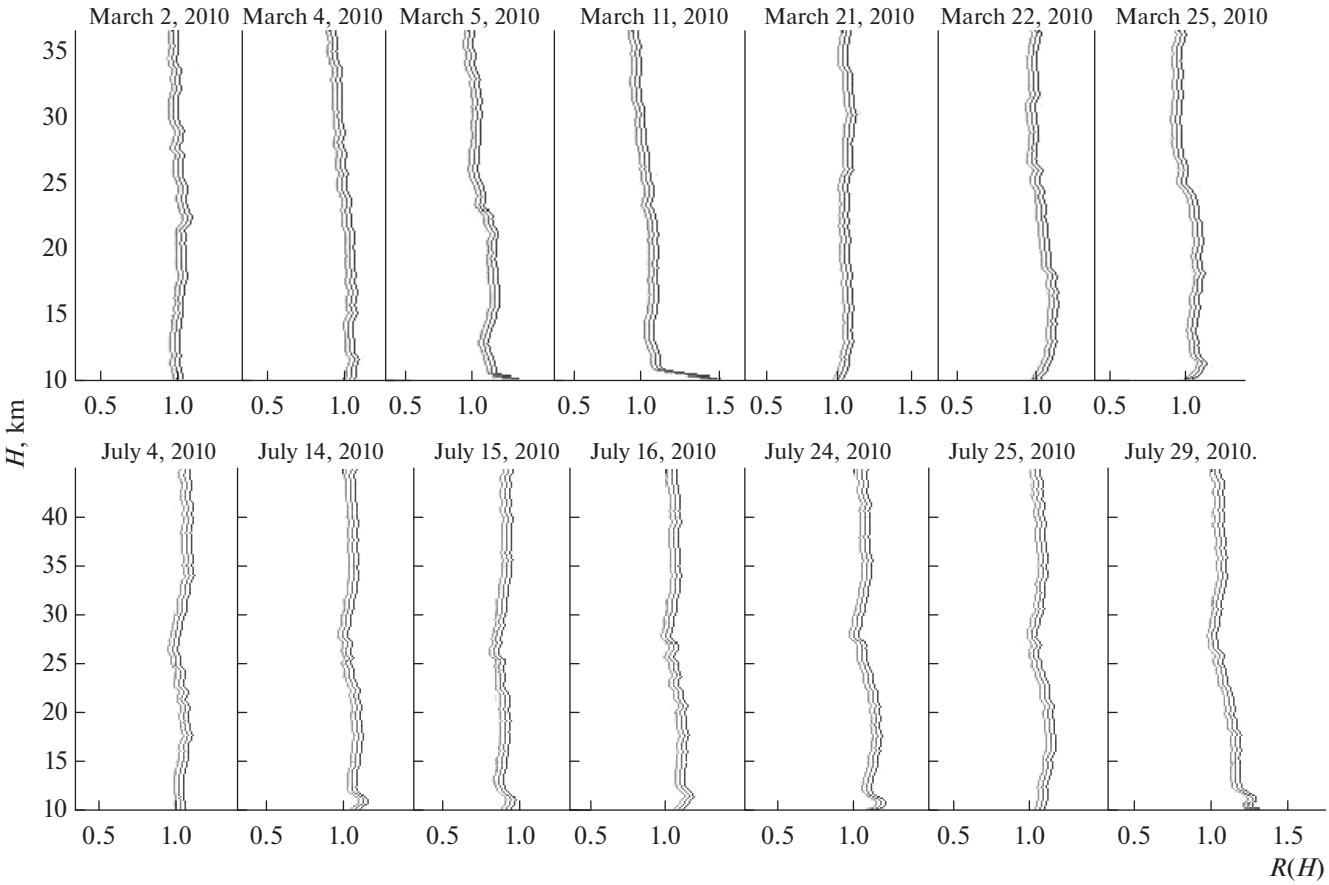

Fig. 11. Vertical profiles of scatter ratio over Tomsk observed in quiet postvolcanic period in March and July 2010. No profiles are shown for the April–June period, because they are completely analogous to those presented above. From *R(H)* values close to the unity, it follows that aerosol is almost absent within the observed 10–35 km height interval, i.e., the Junge layer disappeared [11].

ments with the above-indicated accuracy characteristics are possible both in the nighttime and daytime.

ACKNOWLEDGMENTS

The work was supported by a grant from the RF President (NSh4714.2014.5), a Russian National Foundation grant (no. 14-27-00022) to create a receiver for combined light scattering, and the Program "D. I. Mendeleev Scientific Foundation of Tomsk State University" in 2014–2015 (project no. 8.2.32.2015).

REFERENCES

1. McClatchey, R.A., Fenn, F.W., Selby, J.E., Volz, F.E., and Garing, J.S., *Optical Properties of the Atmosphere*, Air Force Cambridge Research Laboratories, 1971, AFCRL-71-0279, Environ. Res. Pap. no. 354.
2. Angot, G. and Keckhut, Ph., Hauchecorne, A., and Claud, Ch., Contribution of stratospheric warmings to temperature trends in the middle atmosphere from the lidar series obtained at Haute-Provence Observatory (44°N), *J. Geophys. Res.*, 2012, vol. 117, D21102.
3. Zann, U., Cossart, G., Fiedler, J., et al., The ALOMAR Rayleigh/Mie/Raman lidar objectives, configuration, and performance, *Ann. Geophys.*, 2000, no. 18, pp. 815–833.
4. Balin, Yu.S. and Tikhomirov, A.A., The history of development and operation of the first Russian space lidar BALKAN integrated into Mir space station, *Opt. Atmos. Okeana*, 2011, vol. 24, no. 12, pp. 1078–1087.
5. Burlakov, V.D., Dolgii, S.I., Nevzorov, A.V., et al., Traces of eruption of Eyjafjallajökull volcano according to data of lidar observations in Tomsk and Surgut, *Atmos. Oceanic Opt.*, 2012, vol. 25, no. 2, pp. 110–117.
6. Burlakov, V.D., Dolgii, S.I., and Nevzorov, A.V., Lidar observations of the stratosphere aerosol disturbances over Tomsk (56.5°N; 85.0°E) in period of volcanic activity of 2006–2010, *Opt. Atmos. Okeana*, 2011, vol. 24, no. 12, pp. 1031–1040.
7. Bychkov, V.V., Perezhogin, A.S., Shevtsov, B.M., et al., Accounting for pulses of photomultiplier tube aftereffect in lidar signals of the Kamchatka middle atmosphere, *Opt. Atmos. Okeana*, 2011, vol. 24, no. 2, pp. 107–113.
8. Bychkov, V.V., Perezhogin, A.S., Perezhogin, A.S., et al., Lidar observations of aerosol occurrence in the

middle atmosphere of Kamchatka in 2007–2011, *Atmos. Oceanic Opt.*, 2012, vol. 25, no. 3, pp. 228–235.

9. Bychkov, V.V., Shevtsov, B.M., and Marichev, V.N., Some statistically average characteristics of occurrence of aerosol scattering in the middle atmosphere of Kamchatka, *Atmos. Oceanic Opt.*, 2013, vol. 26, no. 2, pp. 104–106.
10. Marichev, V.N., Lidar investigations of stratospheric warming events above Tomsk in 2008–2010, *Opt. Atmos. Okeana*, 2011, vol. 24, no. 5, pp. 386–391.
11. Marichev, V.N., Investigation into features of manifestation of winter stratospheric warming events over Tomsk from the data of lidar temperature measurements in 2010–2011, *Opt. Atmos. Okeana*, 2011, vol. 24, no. 12, pp. 1041–1046.
12. Marichev, V.N., Investigation of variability of the background aerosol vertical structure above Tomsk based on lidar observations in 2010–2011, *Opt. Atmos. Okeana*, 2012, vol. 25, no. 11, pp. 976–984.
13. Marichev, V.N., Matvienko, G.G., Lisenko, A.A., et al., First results of an integrated experiment on sounding the middle atmosphere in optical and millimeter wavelength ranges (over Tomsk), *Atmos. Oceanic Opt.*, 2013, vol. 26, no. 3, pp. 222–226.
14. Marichev, V.N. and Samokhvalov, I.V., Lidar observations of aerosol volcanic layers in stratosphere of Western Siberia in 2008–2010, *Opt. Atmos. Okeana*, 2011, vol. 24, no. 3, pp. 224–231.
15. Pavlov, A.N., Stolyarchuk, S.Yu., Shmirko, K.A., and Bukin, O.A., Lidar measurements of variability of the vertical ozone distribution caused by the stratosphere–troposphere exchange in the Far East Region, *Opt. Atmos. Okeana*, 2013, vol. 26, no. 2, pp. 126–134.
16. Cheremisin, A.A., Marichev, V.N., and Novikov, P.V., Lidar observations of volcanic aerosol content in the atmosphere over Tomsk, *Russ. Meteorol. Hydrol.*, 2011, vol. 36, no. 9, pp. 600–607.
17. Marichev, V.N. and Bochkovskii, D.A., Lidar measurements of air density in the middle atmosphere. Part 1. Modeling of the potential capabilities in the visible spectral range, *Opt. Atmos. Okeana*, 2013, vol. 26, no. 7, pp. 553–563.
18. Ippolitov I.I., Komarov V.S., and Mitsel', A.A., An opticometeorological model of the atmosphere for simulating lidar measurements and calculating radiation transfer, in *Spektrometricheskie metody zondirovaniya atmosfery* (Spectrometric Methods of Atmospheric Sounding), Novosibirsk: Nauka, 1985, pp. 4–44.
19. Dozier, J., A clear-sky spectral solar radiation model for snow-covered mountainous terrain, *Water Resour. Res.*, 1980, vol. 16, no. 4, pp. 709–718.
20. Zuev, V.E. and Komarov, V.S., *Statisticheskie modeli temperatury i gazovykh komponent atmosfery* (Statistical Models of Temperature and Gas Components of the Atmosphere), Leningrad: Gidrometeoizdat, 1986.
21. Molina, L.T. and Molina, M.J., Absolute absorption cross sections of ozone in the 185–150 nm wavelength range, *J. Geophys. Res.*, 1986, vol. 91, no. 13, pp. 14501–14508.
22. Zuev, V.E., *Rasprstranenie vidimykh i infrakrasnykh voln v atmosfere* (Propagation of Visible and Infrared Waves in the Atmosphere), Moscow: Sovetskoe radio, 1970.
23. Purmal', A.P., Stratified sky, *Khim Zhizn., XXI Vek*, 2005, no. 8, pp. 20–21.
24. Zuev, V.V., Zuev, V.E., and Marichev, V.N., Observations of the stratospheric aerosol layer due to Mt. Pinatubo eruption at a network of lidar stations, *Opt. Atmos. Okeana*, 1993, vol. 6, no. 10, pp. 1180–1201.
25. Burlakov, V.D., El'nikov, A.V., Zuev, V.V., et al., Traces of the Pinatubo volcano eruption in the stratosphere over Western Siberia, *Opt. Atmos. Okeana*, 1992, vol. 5, no. 6, pp. 379–380.
26. Collins, R.L., Polar stratospheric clouds at South Pole in 1990: Lidar observations and analysis, *J. Geophys. Res.*, 1991, vol. 98, no. D1, pp. 1001–1010.
27. Khromov, S.P. and Mamontova, L.I., *Meteorologicheskii slovar'* (Meteorological Dictionary), Leningrad: Gidrometeoizdat, 1974.
28. Marichev, V.N. and Ilyushik, V.Yu., Variability of the aerosol vertical structure in the stratosphere over Tomsk according to lidar observations in 2011, in *Sbornik dokladov 18-go mezhdunarodnogo simpoziuma "Optika atmosfery i okeana. Fizika atmosfery"* (Proceedings of the 18th International Symposium "Atmospheric and Oceanic Optics. Atmospheric Physics"), Irkutsk, 2012, pp. D-78–D-82.
29. El'nikov, A.V., Krekov, G.M., and Marichev, V.N., Lidar observations of the stratospheric aerosol layer over Western Siberia, *Izv. Akad. Nauk: Fiz. Atmos. Okeana*, 1988, vol. 24, no. 8, pp. 818–823.
30. Ivanov, V.N., Zubachev, D.S., Korshunov, V.A., et al., Lidar observations of stratospheric aerosol traces of Chelyabinsk meteorite, *Opt. Atmos. Okeana*, 2014, vol. 27, no. 2, pp. 117–122.
31. Cheremisin, A.A., Marichev, V.N., and Novikov, P.V., Transport of polar stratospheric clouds from the Arctic to Tomsk in January 2010, *Atmos. Oceanic Opt.*, 2013, vol. 26, no. 6, pp. 492–498.

Translated by A. Danilov

SPELL: 1. warmings